Precipitation regime and stable oxygen isotopes at Dome C, East Antarctica – a comparison of two extreme years 2009 and 2010

E. Schlosser[1,2], B. Stenni[3], M. Valt[4], A. Cagnati[4], J. G. Powers[5], K. W. Manning[5], M. Raphael[6], and M. G. Duda[5]

[1] {Inst. of Atmospheric and Cryospheric Sciences, University of Innsbruck, Innsbruck, Austria}

[2] {Austrian Polar Research Institute, Vienna, Austria}

[3] {University of Venice, Venice, Italy}

[4] {Avalanche Service Arabba, Italy}

[5] {National Center for Atmospheric Research, Boulder, CO, USA}

[6] {Department of Geography, University of California, Los Angeles, California, USA}

submitted to: Atmospheric Chemistry and Physics

18 September 2015

revised version for ACPD 13 October 2015

revised version after review 10 February 2016

Correspondence to: E. Schlosser (Elisabeth.Schlosser@uibk.ac.at)

Abstract

At the East Antarctic deep ice core drilling site Dome C, daily precipitation measurements have been initiated in 2006 and are being continued until today. The amounts and stable isotope ratios of the precipitation samples as well as crystal types are determined. Within the measuring period, the two years 2009 and 2010 showed striking contrasting temperature and precipitation anomalies, particularly in the winter seasons. The reasons for these anomalies are analysed using data from the mesoscale atmospheric model WRF (Weather Research and Forecasting Model) run under the Antarctic Mesoscale Prediction System (AMPS). 2009 was relatively warm and moist due to frequent warm air intrusions connected to amplification of Rossby waves in the circumpolar westerlies, whereas the winter of 2010 was extremely dry and cold. It is shown that while in 2010 a strong zonal atmospheric flow was dominant, in 2009 an enhanced meridional flow prevailed, which increased the meridional transport of heat and moisture onto the East Antarctic plateau and led to a number of high-precipitation/warming events at Dome C. This was also evident in a positive (negative) SAM (Southern Annular Mode) index and a negative (positive) ZW3 (Zonal Wave number three) index during the winter months of 2010 (2009). Changes in the frequency or seasonality of such event-type precipitation can lead to a strong bias in the air temperature derived from stable water isotopes in ice cores.

1 Introduction

Although Antarctic precipitation has been studied for approximately half a century (see e.g. Bromwich, 1988), a number of open questions remain. There are two key motivations for studying Antarctic precipitation. The first is that precipitation/snowfall is the most important positive component of the mass balance of Antarctica. This is receiving increasing attention in discussions of climate change since the mass balance response to global warming can considerably influence sea level change. A possible increase of precipitation in a future climate due to higher air temperatures and therefore increased saturation vapour pressure would mean storage of larger amounts of water in the Antarctic ice sheet, thus mitigating sea level rise (Church et al., 2013*)*. So far, the expected increase in precipitation has not been

found in the measurements (e.g. Monaghan et al., 2006). However, in one projection derived from a combination of various models and ice core data, Frieler et al. (2015) state a possible increase in Antarctic accumulation on the continental scale of approximately 5% K^{-1}. In some parts of Antarctica, higher accumulation would lead to increased ice flow and thus dynamical ice loss, which would reduce the total mass gain (Harig and Simons, 2015; Winkelmann et al., 2012). Thus, for calculation of the Antarctic mass balance, precipitation amounts and precipitation regimes have to be known as exactly as possible.

A second driver for studying Antarctic precipitation is that the ice of Antarctica is an unparalleled climate archive: ice cores up to 800.000 years old yield crucial information about palaeotemperatures and the past constitution of the atmosphere (e.g. EPICA community members, 2004). To derive former air temperatures from ice cores, the stable-isotope ratios of water are used primarily. A linear spatial relationship has been found between mean annual stable isotope ratios in Antarctic precipitation and annual mean air temperature at the deposition site although the isotope ratios depend in a complex way on mass-dependent fractionation processes during moisture transport and precipitation formation (Dansgaard, 1964). Since the heavier isotopes have a lower saturation vapour pressure than the lighter ones, they condense more easily and evaporate less rapidly. The molecular diffusivity is smaller for the heavier isotope, ^{18}O, than for ^{16}O as well. This is equally valid for hydrogen and its heavier stable isotope deuterium (D). Therefore, the isotope ratio changes during evaporation and condensation processes. When an air mass is cooled (on the transport south to Antarctica or in ascent to higher elevations) it gets increasingly depleted in the heavier isotopes (^{18}O and D) because they preferably fall out as precipitation. The amount of this fractionation depends on the difference between the condensation temperature close to the initial moisture source and that at the final deposition site (Jouzel et al., 2003; 2014). Since the annual temperature amplitude is larger on the continent than in the maritime climate of the Southern Ocean, the ^{18}O values are lower during cold periods (winter/glacial) than during warm periods (summer/interglacial), which leads to clear seasonal variations and likewise large differences between glacial and interglacial periods in the stable isotope ratios measured in the ice core.

This spatially derived linear relationship has been found not to hold temporally, however (Jouzel et al., 2003). Apart from air temperature, several other factors influence the stable isotope ratio, such as seasonality of precipitation, location of and conditions at the moisture sources and conditions along moisture transport paths (e.g. Sodemann and Stohl, 2009;

Sodemann et al., 2008, Jouzel et al., 2003; Noone et al., 1999; Schlosser, 1999). Thus, for a correct interpretation of the ice core data a thorough understanding of the atmospheric processes responsible for the precipitation is needed, as it was the precipitation that ultimately formed the glacier ice investigated in the cores. In particular, information about moisture sources, moisture transport paths, and atmospheric conditions at the final deposition site is required.

Measuring Antarctic precipitation is a challenge, not only due to the remoteness and extreme climate of the continent, but also due to difficulties in distinguishing between drifting/blowing snow and falling precipitation. The latter is due to the high wind speeds that typically accompany precipitation events in coastal areas. In the interior of the continent, while wind speeds are lower than at the coast, the threshold for drifting snow is often lower due to lower snow densities as well. Measurements are also complicated by the extremely small amounts of precipitation produced in the cold and dry air. Precipitation measurements with optical devices may hold some hope for improved data in the future, but these instruments are currently in the testing phase in Antarctica (Colwell, pers. comm.). In light of the lack of observations, atmospheric models have become increasingly useful tools to investigate Antarctic precipitation (Bromwich et al., 2004; Schlosser et al., 2010a; 2010b; 2008; Noone and Simmons, 2002; Noone et al., 1999; Noone and Simmons, 1998).

This study focusses on the differences in the precipitation regime of two contrasting years within the short measuring period, motivated by the consequences different precipitation/flow regimes have on stable isotope interpretation. The stable istopes themselves are only discussed as additional information about the local conditions in the respective years and will be topic of a different study. The present investigation concentrates on the years 2009 and 2010. These years were chosen because they showed striking contrasting temperature and precipitation anomalies, particularly in the winter seasons. Fogt (2010) reports that temperatures in the Antarctic were persistently above average in the mid-to-lower troposphere during the winter of 2009. The positive surface temperature anomalies were most marked in East Antarctica. In 2010, the picture was very different from 2009, with generally below-average temperatures on the East Antarctic plateau in winter and spring (Fogt, 2011).

2 Study site

Dome C (75.106 °S, 123.346 °E, elevation 3233m) is one of the major domes on the East Antarctic ice sheet. Its mean annual temperature is -54.5 °C, and the mean annual accumulation derived from ice cores amounts to 25 mm water equivalent (w.e)./yr. Several deep ice cores have been retrieved at Dome C, the first one in 1977/78, reaching a depth of 906 m, corresponding to an age of approximately 32,000 yr. The thermally drilled core was retrieved during the International Antarctic Glaciological Project (Lorius, 1979).

The oldest ice to date has been obtained at Dome C through the European deep drilling project EPICA (European Project for Ice Coring in Antarctica). The drilling was completed in January 2006; at the base of the 2774.15 m long ice core the age of the ice was estimated to be 800.000 yr, thus covering eight glacial cycles (EPICA community members, 2004). To support the EPICA drilling operation, the French-Italian Antarctic wintering base Dome Concordia became operational in 2005.

3 Previous work

3.1 Large-scale circulation patterns and precipitation

Precipitation conditions in the interior of Antarctica are very different from those in coastal areas. Whereas precipitation at the coast is usually caused by frontal systems of passing cyclones that form in the circumpolar trough (e.g. Simmonds et al., 2002), in the interior different precipitation mechanisms are at play. On the majority of days, only diamond dust, also called clear-sky precipitation, is observed. It forms due to radiative cooling in a nearly saturated air mass. Although diamond dust is predominant temporally, it does not necessarily account for the largest fraction of the total yearly precipitation. It has been shown that a few snowfall events per year can bring up to 50% of the total annual precipitation (Braaten et al., 2000; Reijmer and van den Broeke, 2003; Fujita and Abe, 2006; Schlosser et al., 2010a; Gorodetskaya et al., 2013). Those events are due to amplification of Rossby waves in the circumpolar westerlies, which increases the meridional transport of heat and moisture polewards. In extreme cases this can even mean a transport from the Atlantic sector across the continent to the Pacific side (Sinclair, 1981; Schlosser et al., 2015b) The relatively moist and warm air is orographically lifted over the ice sheet, followed by cloud formation and/or

precipitation (Noone et al, 1999; Massom et al., 2004; Birnbaum et al., 2006; Schlosser et al., 2010). Except for the study by Fujita and Abe (2006), all of these investigations were based on model and AWS data, rather than daily precipitation measurements.

For a long time it was believed in ice core studies that precipitation represented in Antarctic ice cores is formed close to the upper boundary of the temperature inversion layer assuming that the largest moisture amounts are found where the air temperature is highest (Jouzel and Merlivat, 1984). This is a very simplified view that is, however, widely used in ice core studies. It assumes that there are basically no multiple temperature inversions and that humidity is only dependent on temperature through the Clausius-Clapeyron equation, which describes the temperature dependence of vapour pressure. This would mean that humidity and temperature inversions would always have a similar profile. However, more recent studies have shown that humidity inversions are parallel to the temperature inversion only in 50% of the cases, and often multiple humidity (and temperature) inversions occur (Nygard et al., 2013). In particular, the local cycle of sublimation and re-sublimation (deposition) is poorly known, but it is important for both mass balance and isotope fractionation studies.

At Dome Fuji, at an elevation of 3810m, the air can be so dry that, in spite of the advection of warm and moist air related to amplified Rossby waves, no precipitation is observed at the site. However, this synoptic situation can cause a strong warming in the lower boundary layer (particularly during blocking situations) due to a combination of warm air advection and removal of the temperature inversion layer by increased wind speed that induces mixing and cloud formation, which in turn increases downwelling longwave radiation (Enomoto et al, 1998; Hirasawa et al., 2000). Increased precipitation amounts can also be observed after a snowfall event when the warm air advection has ended, but increased levels of moisture prevail, which can lead to extraordinarily high amounts of diamond dust precipitation (Hirasawa et al., 2013). In West Antarctica, intrusions of warm, marine air can lead to increased cloudiness, precipitation and air temperature. A change in the frequency or intensity of such warm air intrusions could have a large effect on West Antarctic climate if the mean general circulation changed (Nicolas and Bromwich, 2011).

Moisture origin has been investigated in various studies using back-trajectory calculations employing different models and methods (Scarcilli et al., 2010; Sodemann and Stohl, 2009; Sodemann et al. 2008; Suzuki et al., 2008; Reijmer et al., 2002). In a recent study by Dittmann et al. (2015), who investigated precipitation and moisture sources at Dome F for precipitation events in 2003, it was estimated that the origin of the moisture was farther south

(on average at 50°S) and the transport occurred lower in the atmosphere (approximately at the 500-hPa level) than previously assumed in ice core studies. Since the humidity calculated along the 300hPa-trajectory was already comparatively low (absolute humidity a factor 10 lower at 300hPa than at 500hPa) we assume the 500hPa level as representative for the main moisture flow, which is, of course, not restricted to the 500hPa level, but occurs in a thicker layer that includes the 500hPa level.

3.2 Stable isotopes

Dome C is a deep ice core drilling site. However, the measurements presented here are the first derived from fresh snow samples at this site. A similar study, if only for a period of approximately one year, was carried out by Fujita and Abe (2006) at Dome Fuji (see Fig. 1), another deep-drilling site in East Antarctica. They investigated daily precipitation data together with measurements of stable isotope ratios of the precipitation samples. Temporal variations of $\delta^{18}O$ were highly correlated with air temperature. The lowest $\delta^{18}O$ value measured was –81.9 ‰, which is the isotopically lightest water ever collected on the Earth's surface. Half of the annual precipitation resulted from only 11 events (18 days), without showing any seasonality. The other half was due to diamond dust. Similar results were found in studies by Schlosser et al. (2010a), at Kohnen Station (see Fig. 1) and by Reijmer and Van den Broeke (2003), who used data from automatic weather stations in Dronning Maud Land. The precipitation-weighted temperature was significantly higher than the mean annual surface temperature because the precipitation events were related to warm-air advection, which leads to a warm bias in the $\delta^{18}O$ record. Recently, Dittmann et al. (2015) investigated the stable isotope data obtained by Fujita and Abe (2006) at Dome Fuji for all days with dynamically caused snowfall in a combined approach of synoptic analysis and isotope modelling. They found that, for single events, the relationship between deuterium excess and atmospheric conditions at the moisture source used in ice core studies was not existent.

4 Data and methods

4.1 Precipitation and isotopes

Daily precipitation measurements were initiated at Dome C in 2006, and have, with some interruptions, been continued until today. Daily precipitation amounts are measured using a wooden platform set up at a distance of 800 m from the main station, at a height of 1 m above the snow surface to avoid contributions from low drifting snow. For the same reason, the platform is surrounded by a rail of approximately 8 cm height. The measurements include precipitation sampling and analysis of stable water isotopes ($\delta^{18}O$, δD) of the samples. Additionally the crystal structure of the precipitation is analysed in order to distinguish between diamond dust, snowfall, and drift snow. Diamond dust consists of extremely fine ice needles whereas synoptic snowfall shows various types of regular snow crystals, which tend to be broken in case of drifting/blowing snow. The snow crystal type depends on air temperature during formation in the cloud. Samples of mixed crystal types can also occur.

While errors of the precipitation measurements cannot be quantified, it is understood that they can exceed 100% given the extremely small precipitation amounts.

The snow samples were sent to the Geochemistry Laboratory of the University of Trieste, where they were melted and stored in freezers at approximately -20 °C until, provided the precipitation amount was sufficient, they were analysed using a mass spectrometer (Thermo-Fisher Delta Plus XP). Very small samples were analysed using a Picarro I1102-I cavity-ringdown spectroscopy (CRDS) analyser. The precision of the Picarro I1102-I is 0.1 ‰ for $\delta^{18}O$ and 0.5 ‰ for δD (Stenni et al., 2015). Details of the measurements and an extensive discussion of the full data set can be found in Stenni et al. (2015)

The Dome C precipitation series is the first and so far only multi-year precipitation/stable isotope series at an Antarctic deep ice core drilling site.

4.2 AWS data

The Antarctic Meteorological Research Center (AMRC) and Automatic Weather Station (AWS) Program are sister projects of the University of Wisconsin-Madison funded under the United States Antarctic Program (USAP) that focus on data for Antarctic research support,

providing real-time and archived weather observations and satellite measurements and supporting a network of automatic weather stations across Antarctica.

The current AWS at Dome C was set up by the AMRC, in December 1995. The station measures the standard meteorological variables of air temperature, pressure, wind speed, wind direction, and humidity. Data can be obtained from http://amrc.ssec.wisc.edu. Note that an initial AWS (named Dome C) had been set up in 1985, however, at a distance of about 70 km from the current site. Thus, only data from the new station (Dome C II) are used in the present study.

4.3 WRF Model Output from the AMPS Archive

In addition to the observations described above, this study uses numerical weather prediction (NWP) model output for analysis of the synoptic environments of the target years, of precipitation processes, and of events. The output is from forecasts of the Weather Research and Forecasting (WRF) Model (Skamarock et al., 2008) run under the Antarctic Mesoscale Prediction System (AMPS) (Powers et al., 2003; 2012), a real-time NWP capability that supports the weather forecasting for the United States Antarctic Program (USAP). The (U.S.) National Center for Atmospheric Research (NCAR) has run AMPS since 2000 to produce twice-daily forecasts covering Antarctica with model grids of varying resolutions. The AMPS WRF forecasts have been stored in the AMPS Archive and used extensively in studies (e.g. Monaghan et al., 2005; Seefeldt and Cassano, 2008; Schlosser et al., 2008; Seefeldt and Cassano, 2012). For 2009 and 2010, the WRF output over the Dome C region reflects a forecast domain with a horizontal grid spacing of 15 km, employing 44 vertical levels between the surface and 10 hPa. This 15-km grid was nested within a 45-km grid covering the Southern Ocean, and Fig. 2 shows these domains.

Model output from AMPS has been verified through various means over the years. Multi-year AMPS forecast evaluations have been conducted (Bromwich et al., 2005), and WRF's ability for the Antarctic in particular has been confirmed (Bromwich et al., 2013). AMPS's and WRF's Antarctic performance has also been documented in a number of case and process studies (e.g. Bromwich et al., 2013; Nigro et al., 2011; 2012; Powers, 2007). For model development within AMPS, verification for both warm and cold season periods is performed

prior to changes in model versions or configurations (Powers et al., 2012). The reliability of AMPS WRF forecasts is also reflected in their demand from international Antarctic operations and field campaign forecasting efforts (see e.g. Powers et al., 2012). Lastly, similarly to how it is used here, AMPS output has been a key tool in previous published studies of Antarctic precipitation related to ice core analyses (Schlosser et al., 2008; 2010a; 2010b).

In this study the WRF output from the AMPS archive is used to study both the synoptic patterns and the local conditions related to the precipitation regimes and events in the years compared. The WRF forecasts provide reliable depictions of conditions and their evolution, and are used for trajectories and estimates of precipitation source and type. This includes information on temperatures (in both source and deposition areas) and precipitation.

5 Results

5.1 Temperature and precipitation

Figure 3a shows the mean monthly air temperature observed at the Dome C AWS for 2009 and 2010 as well as the mean of 1996-2014. The mean annual cycle exhibits the typical coreless winter (van Loon, 1967) with a distinct temperature maximum in summer (December/January), which has no counterpart in winter, where the months May to August show relatively similar values. This is due to a combination of the local surface radiation balance and warm air intrusions. During the first part of the polar night, with the lack of short-wave radiation, anequilibrium of downwelling and upwelling longwave radiation is reached; advection of relatively warm air from lower latitudes further reduces the possibility for cooling. Thus the temperature does not decrease significantly after May (King and Turner, 1997; Schwerdtfeger 1984).

Whereas during the summer months little difference is seen between 2009 and 2010 the winter months are strikingly different. The lowest mean July temperature of the station record occurs in 2010 with a value of -69.7 °C. This is the lowest monthly mean ever observed at Dome C, 5.9 °C lower than the average 1996-2014, corresponding to a deviation of

1.7σ, σ being the standard deviation. In contrast, the highest July mean temperature is found in 2009; with a value of -54.9 °C, it was 8.9 °C higher (corresponding to 2.5σ) than the long-term July mean and the only July mean that exceeded -60 °C. In Figure 3b, observed daily mean temperatures and daily precipitation sums for the years 2009 and 2010 are displayed. Again, the differences between the two years are most striking in winter. In 2009, the temperature variability is very high, and several warming events with temperatures up to almost -30 °C can be seen. Minimum temperatures are rarely lower than -70 °C whereas in 2010, minima are close to -80 °C. The highest temperature in the winter of 2010 was only slightly above -50 °C. The winter 2009 thus was not only a "coreless winter", but had a "warm" core due to the high number of warm air intrusions.

A very high value precipitation value of 1.36 mm on 9 February 2010, followed by 0.67 mm on 10 February, both classified as diamond dust from the photographic crystal analysis, stems from only one event around 9 February. These values should be considered with care given the high error possibilities of the measurements. Considering the extremely low density of diamond dust, a diamond dust amount of more than 1mm/day seems to be unlikely. However, the model data do show a precipitation event connected to warm air advection from the north (see below) for this day, which would indicate the occurrence of snowfall rather than diamond dust. Most likely a mixture of crystal types was found during this event with the diamond dust on top of the snow crystals, which possibly led to the classification of the event as diamond dust. (Note that the crystal classification was carried out purely from photographs by an expert at the Avalanche Institute in Italy and that snow crystals are also comparatively small at the temperatures prevailing at Dome C). The precipitation totals for May to September are 12.0 mm w.e. for 2009 and 4.3 mm w.e. for 2010. Daily sums exceed 0.25 mm only three times in 2010, but 16 times in 2009. Usually, high daily precipitation amounts are associated with relative maxima in air temperature. In general, the winter of 2010 was cold and dry, whereas 2009 was relatively warm and moist compared to the long-term average.

Figure 4a shows monthly precipitation amounts for 2009 and 2010, distinguishing between diamond dust, hoar frost, and snowfall; Figure 4b gives the relative frequencies of the three different observed types of precipitation for both years. Again, large differences between 2009 and 2010 are found. While approximately half of the precipitation fell as snow in 2009, less than a quarter of the total precipitation stemmed from snowfall in 2010, when mostly diamond dust was observed. As seen before, the winter months of May to September exhibit the largest differences. In particular, the extremely "warm" July of 2009 brought high amounts of

snowfall. The lowest amounts of precipitation are seen in austral summer 2009/2010, with no precipitation observed in November and only very small amounts in December and January.

The total amount of precipitation measured on the raised platform is 16.5 mm w.e. for 2009 and 13.4 mm w.e. for 2010, compared to the mean annual accumulation of 25 mm w.e. derived from firn core and stake measurements (Frezzotti et al., 2005). From the available data it cannot be determined whether the difference is due to snow removed from the measuring platform by wind or sublimation or snow added to the snow surface by wind (blowing or drifting snow) or deposition (re-sublimation).

5.2 Atmospheric flow conditions

5.2.1 Synoptic analyses with AMPS archive data

The synoptic situations that caused precipitation at Dome C were analysed using WRF output data from the AMPS archive. In particular, fields of 500hpa geopotential height and 24-h precipitation were used. For the 500hPa geopotential height information the 12-h forecast was utilized. For 24-h precipitation, the 12-36h forecast sums of precipitation (rather than 0-24h) were used to allow for model spin up of clouds and microphysical fields. This is considered long enough for moist process spin-up, but avoids error growth reflected in longer forecast times (Bromwich et al., 2005).

For all precipitation events with observed daily sums exceeding 0.2mm, the synoptic situations that caused the precipitation were investigated. In total, 29 events were studied, 20 in 2009 and 9 in 2010. For 2009 (2010), the model showed precipitation at Dome C in 44% (50%) of the studied cases and precipitation in the vicinity in 33 (25) % of the cases; no precipitation was shown in the model in 22 (25) % of the cases. In total, approximately half of the precipitation events were represented well by the model, one quarter showed synoptic events that did not bring precipitation exactly at the location and time of the measurements, and one quarter of the cases were not forecast by the model at all. An exact quantitative analyis of the model skill using the entire data series starting in 2006 is ongoing and the results will be more meaningful than those of only two, not very typical, years.

Generally, snowfall events were found to be associated with an amplification of the Rossby waves in the circumpolar westerlies, which causes a northerly flow across the Dome C region between a trough to the west and an upper-level ridge to the east of Dome C. This northerly

flow brings relatively warm and moist air from as far as 35 °S - 40 °S to the East Antarctic plateau, leading to orographic precipitation when it is forced to ascende on the way from the coast to the high-altitude interior. Variations of this general situation are due to the duration of the flow pattern (e.g. whether there is a blocking anticyclone or not) and the strength of the upper-level ridge, which determines how far north the main moisture origin is situated. Figure 5 shows an example of this synoptic situation typical for snowfall events. In the 500hPa geopotential height field (Fig. 5a) for 13 September 2009 the amplified ridge that leads to a northerly flow towards Dome C can be seen slightly east of Dome C, with an axis tilted in a NE-SW direction. Figure 5b displays the 24-h precipitation caused by the N-NE flow onto the continent. Dome C is situated at the southeastern edge of the precipitation area.

Using the WRF output, three-dimensional 5-day back-trajectories were calculated for for arrival levels of 300hPa, 500hPa, and 600hPa (Fig. 5c) for this event. These levels were chosen as 600 hPa is close to the surface of Dome C (note that surface pressure can be lower than 600hPa at times, too), while 500hPa and 300hPa yield information about the large-scale atmospheric flow. The trajectories were calculated with the graphics software RIP. RIP stands for "**R**ead/**I**nterpolate/**P**lot" and is a Fortran program that invokes NCAR Graphics routines for the purpose of visualizing output from gridded meteorological data sets, which includes trajectory calculations (Stoelinga, 2009). The three-dimensional displacement of an air parcel during a time step Δt is calculated using an iterative scheme:

$$X_{n+1} = X_0 + \Delta t/2\,[v(X_{0,t}) + v\,(X_{n,t} + \Delta t)], \qquad \text{(Eq. 1)}$$

where Δt is the iteration time step, X_0 the position vector of the parcel at time t, X_n the n^{th} iterative approximation of the position vector at time $t + \Delta t$ and $v(X,t)$ the wind vector at position X and time t. The time step we used was 600s. For simplicity's sake, RIP does not define a threshold for convergence, but simply does two iterations for each time step, which turned out to be exact enough in the praxis for our purposes. The resolution of the input data corresponds to the resolution of AMPS/WRF during the respective time period. The data are linearly interpolated in time and space. Taking into account the large uncertainties in trajectory calculations, for this case a main moisture source at approximately 40 °S was estimated. Note, that the moisture source is not defined as the location of the trajectory five days previous to the precipitation. Instead, for this estimate, the combined information of the trajectories and the 500hPa geopotential height fields is used. Different from the approach of Sodemann and Stohl (2009) and Sodemann et al. (2008), who calculated 20-day back-trajectories, for a 5-day trajectory it is possible to comprehend the dynamics of the synoptic

situation that causes the precipitation. That way the trajectory results can be cross-checked with the geopotential height fields. Even though the trajectory not explicitely deals with moistuer, it gives information about the origin of the moist air mass. The northernmost "point" of the trough that causes the northerly flow to Dome C is supposed to be the northern limit of the potential moisture source since no substantial meridional flow is observed north of this limit. (The 500hPa trajectory seems to have some inconsistencies (e.g. kinks) on the 5th day, which should not be over-interpreted). Whereas it is not possible to exactly determine the moisture source (under the simplifying assumption of a single moisture source) with this simple method, the information is sufficient to distinguish between a source in the Southern Ocean and one at middle latitudes, which is most important for ice core interpretation and for simple isotope modeling.

A frequent occurrence of the synoptic situation described (as it was the case in 2009) means a more northern mean moisture source than on average, which has to be taken into account for deriving air temperature from stable isotopes. (A detailed study using trajectory calculations for all observed precipitation events at Dome C is ongoing.) It was also found to be typical for precipitation events at Dome C that the main westerly flow is split into a northern branch that remains zonal, whereas the southern branch starts meandering with a strong meriodional component. This is observed more often at Dome C than at Dome F (Dittmann et al., 2015) or at Kohnen Station (Schlosser et al., 2010a).

Figure 6 presents an example for a case with no precipitation in the model, but relatively large observed precipitation amounts. The 500hPa geopotential height field (Fig. 6a) shows a cutoff-high west of Dome C on the day after the precipitation event shown in Figure 5. The remaining atmospheric moisture is not sufficient to produce precipitation in the model (Fig. 6b), but it does lead to remarkably high amounts of diamond dust and/or hoar frost (0.7 mm observed during this event). This synoptic situation was also found by Hirasawa et al. (2013) in a detailed study of the synoptic conditions and precipitation during and after a blocking event at Dome Fuji. (Note that neither diamond dust nor hoar frost formation is specifically parameterized in the model.) In 2010, the flow was mainly zonal and the synoptic situations described above were much less frequent than in 2009 and not as strongly developed.

Using the WRF output, monthly composite fields of 500hPa-geopotential height were calculated to compare the general flow conditions in 2009 and 2010. Figure 7 shows the composite mean 500-hPa geopotential height for July 2009 and 2010, respectively. Even in

441 the monthly mean, the distinct upper-level ridge in 2009 that projects onto the East Antarctic
442 plateau and leads to warm air advection and increased precipitation at Dome C is clearly seen.

443 In 2010, in the monthly average, the flow was mainly zonal, which reduced the meridional
444 exchange of heat and moisture, thus leading to lower temperatures and less precipitation in the
445 interior of the Antarctic continent.

446

447 ### 5.2.2 Southern Annular Mode

448 The occurrence of high-precipitation events on the Antarctic plateau due to amplification of
449 Rossby waves is often connected to a strongly positive phase of the Southern Annular Mode
450 (SAM). The SAM is the dominant mode of atmospheric variability in the extratropical
451 Southern Hemisphere. It is revealed as the leading empirical orthogonal function in many
452 atmospheric fields (e.g. Thompson and Wallace, 2000), such as surface pressure, geopotential
453 height, surface temperature, and zonal wind (Marshall, 2003). Since pressure fields from
454 global reanalyses commonly used to study the SAM are known to have relatively large errors
455 in the polar regions, Marshall (2003) defined a SAM index based on surface observations. He
456 calculated the pressure differences between 40 °S and 65 °S using data from six mid-latitude
457 stations and six Antarctic coastal stations to calculate the corresponding zonal means. A large
458 (small) meridional pressure gradient corresponds to a positive (negative) SAM index . The
459 positive index means strong, mostly zonal westerlies and comparatively little exchange of
460 moisture and energy between middle and high latitudes, which leads to a general cooling of
461 Antarctica, except for the Antarctic Peninsula that projects into the westerlies. A negative
462 SAM index is associated with weaker westerlies and a larger meridional flow component.

463 Figure 8 shows the monthly mean SAM index for 2009 and 2010 (data can be found at
464 http://www.nerc-bas.ac.uk/icd/gjma/sam.html). Whereas in the winter months (May to
465 September) of 2009 the SAM index was generally negative (with the exception of a weakly
466 positive value in June), 2010 has positive indices from April to August, with strongly positive
467 values in June and July, and only a weakly negative index in September. This is consistent
468 with the pattern of a strong zonal flow with few precipitation events at Dome C due to
469 amplified ridges in the winter of 2010, with the opposite situation holding in 2009. The
470 highest SAM index is found in November 2010; however, in austral summer the relationship
471 between the SAM index and precipitation seems to be less straightforward. The differences
472 between 2009 and 2010 are not extraordinarily high compared to other years (e.g. 2001/2002

as seen at http://www.nerc-bas.ac.uk/public/icd/gjma/newsam.spr.pdf), however, qualitatively they are in agreement with the observed flow pattern. Furthermore, it should be kept in mind that SAM explains only about one third of the atmospheric variability in the Southern Hemisphere (Marshall, 2007) and that the SAM index alone gives no information about the location of respective ridges and troughs in a highly meridional flow pattern..

5.2.3 Zonal wave number 3

Another method to investigate the general atmospheric flow conditions is to analyse spatial and temporal variations of the quasi-stationary zonal waves in the Southern Hemisphere. In this study zonal wave number 3 (ZW3) is used. While the atmospheric circulation in the Southern Hemisphere appears strongly zonal (or symmetric), there is a significant non-zonal (asymmetric) component and ZW3 represents a significant proportion of this asymmetry. It is a dominant feature of the circulation on a number of different time scales (e.g. Karoly, 1989), is responsible for 8% of the spatial variance in the field (van Loon and Jenne, 1972), and contributes significantly to monthly and interannual circulation variability (e.g. Trenberth, 1990; Trenberth and Mo, 1985). The asymmetry is revealed when the zonal mean is subtracted from the geopotential height field thereby creating a coherent pattern of zonal anomalies, with the flow associated with these patterns becoming apparent. ZW3 has preferred regions of meridional flow, which influence the meridional transport of heat and moisture into and out of the Antarctic. Raphael (2004) defined an index of ZW3 based on its amplitude (effectively the size of the zonal anomaly) at 50^{o}S showing that ZW3 has identifiable positive and negative phases associated with the meridionality of the flow. A positive value for this index indicates more meridional flow (large zonal anomaly) and a negative value more zonal flow (small zonal anomaly). Note that the ZW3 index used here does not fully capture the shift in phase of the wave. However, Raphael (2004) found that the net effect is a small reduction in the amplitude of the wave, but the sign of the index is not influenced. A new approach for identifying Southern Hemisphere quasi-stationary planetary wave activity that allows variations of both wave phase and amplitutde is described in a recent study by Irving and Simmonds (2015).

Figure 9a shows the monthly mean ZW3 index for the period 2009–2010. From June to September 2009 the ZW3 index was largely positive except for a comparatively small negative excursion in July. On the contrary, from June to September 2010 it was negative. The

asymmetry in the circulation suggested by the index is shown in Figure 9b (July 20090 and 9c (July 2010). These figures were created by subtracting the long-term zonal mean at each latitude, from the mean 500-hPa geopotential height field in July 2009 and 2010, respectively. The flow onto Dome C suggested by the alternating negative and positive anomalies is northerly in July 2009, but has a strong zonal component in July 2010. This information given by the ZW3 index and the patterns of zonal anomalies is consistent with that suggested by the SAM.

5.3 Stable Isotopes

Since the main motivation of the presented precipitation study is the improvement of the climatic interpretation of stable isotope data, in Figure 10 the daily mean temperature and the measured stable isotope ratios of the precipitation samples, namely $\delta^{18}O$ and the second-order parameter deuterium excess d (d= δD-8 $\delta^{18}O$), are displayed for 2009 and 2010. As expected, $\delta^{18}O$ and air temperature exhibit a similar annual cycle, with high values in summer and the lowest values in the winter months. Consistent with the unusually "warm" winter of 2009, also the $\delta^{18}O$ reaches higher values in winter 2009 than in winter 2010. Because of the more meridional flow and thus more northerly (and warmer) oceanic moisture source, the initial $\delta^{18}O$ is already higher than on average and the condensation temperature at Dome C is above-average during the precipitation events as well. In addition to the warm-air advection, the existing near-surface temperature inversion layer is often removed because of increased wind speed and increased cloud cover, the latter causing a change in the radiation balance, namely increased down-welling long-wave radiation. In contrast to $\delta^{18}O$, the deuterium excess shows maxima in winter and minima in summer. In winter 2010, the deuterium excess is clearly higher than in 2009; the difference between the maxima in 2009 and 2010 amounts to 20 **‰**. A comprehensive analysis of the full stable isotope data set of Dome C can be found in a companion paper by Stenni et al. (2015).

6 Discussion and Conclusion

In the present study that was motivated by stable water isotope studies, atmospheric conditionsof the two contrasting years 2009 and 2010 at the Antarctic deep-drilling site Dome

C, on the East Antarctic Plateau were investigated using observational precipitation and temperature data and data from a mesoscale atmospheric model. The observations from Dome C represent the first and only multi-year series of daily precipitation/stable isotope measurements at a deep-drilling site, even though “multi” means only nine years in this case. The differences between the two years 2009 and 2010 were most striking in winter. Whereas 2009 was relatively warm and moist due to frequent warm air intrusions connected to amplification of Rossby waves in the circumpolar westerlies, the winter of 2010 was extremely cold and dry, with the lowest monthly mean July temperature observed since the beginning of the AWS measurements in 1996. This can be explained by the prevailing strong zonal flow in the winter of 2010, related to a strongly positive SAM index and a negative ZW3 index. Also, the frequency distribution of the various precipitation types was largely different in 2009 and 2010, with snowfall prevailing in 2009 whereas diamond dust was dominant in 2010.

Similarly striking differences in weather conditions of 2009 and 2010 were seen in other parts of East Antarctica. Gorodetskaya et al. (2013) found that accumulation in 2009 was eight times higher than in 2010 at the Belgian year-round station “Princess Elisabeth”. At this location, the temperature was also higher in 2009 than in 2010, particularly in fall/early winter. The findings are supported by Boening et al. (2012), who used observations from GRACE (Gravity Recovery And Climate Experiment) and found an abrupt mass increase on the East Antarctic ice sheet in the period 2009-2011. Similarly, Lenaerts et al. (2013) investigated snowfall anomalies in Dronning Maud Land, East Antarctica. They state that the large positive anomalies of accumulation found in 2009 and 2011 stand out in the past approximately 60 years although comparable anomalies are found further back in time.

Distinguishing between the different forms of precipitation, namely diamond dust, hoar frost and dynamically caused snowfall, is important for both mass balance and ice core interpretation. For mass balance, the different precipitation types do not have to be known if the surface mass balance is determined as an annual value from snow pits, firn/ice cores or stake arrays. For temporally higher resolved precipitation measurements, however, a fraction of both hoar frost and diamond dust might be just a part of the local cycle of sublimation and deposition (re-sublimation), thus representing no total mass gain. More detailed measurements are thus necessary to allow a better understanding of the processes involved. This also applies to isotopic fractionation during this cycle; continuous measurements of water vapour stable isotope ratios (e.g. Steen-Larsen et al., 2013) should be included here.

For ice core interpretation, the problem generally becomes more complex. Diamond dust is observed during the entire year without a distinct seasonality. Therefore a signal from an ice core property measured in the ice (in contrast to measured in the air bubbles) will have contributions from diamond dust that stem nearly equally from all seasons. Although snowfall events are not very frequent at deep ice core drilling sites, they can account for a large percentage of the total annual precipitation/accumulation at those locations. If these events have a seasonality that has changed between glacials and interglacials, a large bias will be found in the temperature derived from the stable isotopes in ice cores. Today, the frequency of such snowfall events shows a high inter-annual variability, but both frequency and seasonality of the events might be different in a different climate due to changes in the general atmospheric circulation and in sea ice extent (e.g. Godfred-Spenning and Simmonds, 1996). Since it was found that snowfall events are connected to the synoptic activity in the circumpolar trough, it is plausible that the seasonality of such events was different during glacial times because the sea ice edge and the mean position of the westerlies were considerably farther north than today. This influences the zone of the largest meridional temperature gradient, thus the largest baroclinicity and consequently cyclogenesis. A larger sea ice extent might reduce the number of snowfall events in the Antarctic interior in winter by pushing the zone of largest baroclinicity northwards. However, it is not possible to assess such hypotheses using observational data since the instrumental period, with few exceptions, started in Antarctica with the IGY (International Geopyhysical Year) 1957/58. However, modelling studies can be supported by studies of the physical processes in the atmosphere using recent data, and, in particular, cases of extreme situations can be helpful here. Even if the full amplitude of the change between glacial and interglacial climates is not observed, extrema can give insight into the sign and kind of the reaction of the system to a change in one or several atmospheric variables.

Another implication for ice core interpretation derived from the present study is that a more northern moisture source does not necessarily mean larger isotopic fractionation (which is usually assumed in ice core studies (e.g. Stenni et al., 2001; 2010). Even though the temperature at the main moisture source is higher than on average for a northern moisture source, the depletion in heavy isotopes is comparatively small because the temperature at the deposition site is also clearly higher than on average due to the warm air advection, which reduces the temperature difference between the moisture source region and the deposition site, thus the amount of isotopic fractionation.

Looking towards future work, the results here indicate that a combination of process studies using recent data and modelling of the atmospheric flow conditions on larger time scales will lead to a better quantitative interpretation of ice core data. Apart from the factors influencing precipitation itself, it has become clear recently that post-depositional processes between snowfall events are more important than previously thought because, additionally to processes within the snowpack, the interaction between the uppermost parts of the snowpack and the atmosphere is very intense (Steen-Larsen et al., 2013). Parallel measurements of stable isotope ratios of water vapour and surface now, combined with meteorological data will give more insight into these processes in Antarctica.

Altogether, this means that the relationship between air temperature and stable isotopes of Antarctic precipitation/ice is anything else but straightforward, since the isotope ratio measured in an ice core (or in the snow) is the result of a complex precipitation history that is strongly influenced by the synoptics and general atmospheric flow conditions, followed by post-depositional processes. Without thorough knowledge of all the processes involved a quantitatively correct derivation of paleo temperatures from ice core stable water isotopes is thus not possible.

Author contribution

BS is responsible for the precipitation measurements and stable isotope analysis, MV and AC for the crystal analysis. MR did the ZW3 study. MD and KW assisted with software development. ES prepared the manuscript with contributions from JP, KW, MR, and BS.

Acknowledgements

The precipitation measurements at Dome C as well as the isotopic analysis have been conducted in the framework of the Concordia station glaciology and ESF PolarCLIMATE HOLOCLIP projects funded in Italy by PNRA-MIUR. This is a HOLOCIP publication number xx. The present study is financed by the Austrian Science Funds (FWF) under grant P24223. AMPS is supported by the U.S. National Science Foundation, Division of Polar Programs. We appreciate the support of the University of Wisconsin-Madison Automatic Weather Station Program with the Dome C II data set. (NSF grant numbers ANT-0944018 and

633 ANT-12456663). We thank Gareth Marshall for providing the SAM indices online. We thank
634 all winterers at Dome C, who did the precipitation sampling.

635

636

637 ## References

638

639 Birnbaum, G., Brauner, R., and Ries, H.: Synoptic situations causing high precipitation rates
640 on the Antarctic plateau: observations from Kohnen Station, Dronning Maud Land , Antarctic
641 Science, 18 (2), pp. 279-288, doi: 10.1017/S0954102006000320, 2006.

642 Boening, C., Lebsock, M., Landerer, F., and Stephens, G. : Snowfall-driven mass change on
643 the East Antarctic ice sheet. Geophys. Res. Let., 39, L21501, doi:10.1029/GL053316, 2012.

644 Braaten, D. A.: Direct measurements of episodic snow accumulation on the Antarctic polar
645 plateau. J. Geophysic. Res., 105, (D9) 10,119-10,128, 2000.

646 Bromwich, D. H: Snowfall in high southern latitudes. Rev. Geophys., 26(1) 149-168, 1988.

647 Bromwich, D. H., Guo, Z., Bai, L., and Chen, Q. : Modeled Antarctic Precipitation. Part I:
648 Spatial and Temporal Variability, *J. Climate*, **17**, 427–447, 2004.

649 Bromwich, D. H., Monaghan, A. J., Manning, K. W., and Powers, J. G.: Real-time forecasting
650 for the Antarctic: An evaluation of the Antarctic Mesoscale Prediction System (AMPS), Mon.
651 Weather Rev., 133, 579-603, 2005.

652 Bromwich, D. H., Otieno, F. O., Hines, K. M., Manning, K. W., and Shilo, E.: Comprehensive
653 evaluation of polar weather research and forecasting performance in the Antarctic. J.
654 Geophys. Res., 118, 274–292, doi: 10.1029/2012JD018139, 2013.

655 Church, J.A., et al.: Sea Level Change. In: Climate Change 2013: The Physical Science Basis.
656 Contribution of Working Group I to the Fifth Assessment Report of the Intergovernmental
657 Panel on Climate Change (Stocker, T.F., D. Qin, D., G.K. Plattner, G. K., M. Tignor, M.,
658 Allen, S. K., Boschung, J., Nauels, A., Xia, Y., Bex, V., and Midgley, P. M. (eds.)),
659 Cambridge University Press, Cambridge, United Kingdom and New York, NY, USA, 2013.

660 Dansgaard, W.: Stable isotopes in precipitation, Tellus, XVI (4), 436-468, 1964.

Dittmann, A., Schlosser, E., Masson-Delmotte, V., Powers, J. G., Manning, K. W., Werner, M., and Fujita, K.: Precipitation regime and stable isotopes at Dome Fuji, East Antarctica, Atmos. Chem. Phys. Discuss., doi:10.5194/acp-2015-1012, in review, 2016.Enomoto et al., Winter warming over Dome Fuji, East Antarctica and semiannual oscillation in the atmospheric circulation. J. Geophysic. Res., 103 (D18), 23,103-23,111, 1998.

EPICA community members: 8 Glacial cycles from an Antarctic ice core, Nature, 429, 623-628, doi:10.1038/nature02599, 2004.

Fogt, R. L. In: Arndt, D. S., Baringer, M. O., and M. R. Johnson, Eds., State of the Climate in 2009, 6. Antarctica. Special supplement to Bull. Am. Meteorol. Soc., 91 (7) 125-134, 2010.

Fogt, R. L. In: Blunden, J., Arndt, D. S., Baringer, M. O., Eds., State of the Climate in 2010, 6. Antarctica. Special supplement to Bull. Am. Meteorol. Soc.., 92 (6) 161-172, 2011.

Frezzotti, M., Pourchet, M., Onelio, F., Gandolfi, S., Gay, M., Urbini, S., Vincent, C., Becagli, S., Gragnani, R., Proposito, M., Severi, M., Traversi, R., Udisti, R., and Fily, M.: Spatial and temporal variability of snow accumulation in East Antarctica from traverse data, J. Glaciol., 51(178), 113-123, 2005.

Frieler, K., Clark, P. U., He, F., Buizert, C., Reese, R., Ligtenberg, S.R. M., Van den Broeke, M. R., Winkelmann, R., and Levermann, A.: Consistent evidence of increasing Antarctic accumulation with warming, Nature Climate Change, 5, 348-352, doi:10.1038/NCLIMATE2574, 2015.

Fujita, K., and Abe, O.: Stable isotopes in daily precipitation at Dome Fuji, East Antarctica, Geophys. Res. Lett., 33, L18503, doi:10.1029/2006GL026936, 2006.

Godfred-Spenning, C. and Simmonds, I.: An analysis of Antarctic Sea-Ice and Extratropical cyclone associations. Int. J. Climat., 16, 1315-1332, 1996.

Gorodetskaya, I.V., N.P.M. Van Lipzig, M. R. Van den Broeke, A. Mangold, W. Boot, and C. H. Reijmer: Meteorological regimes and accumulation patterns at Utsteinen, Dronning Maud Land, East Antarctica: Analysis of two contrasting years. J. Geophys. Res, 118, 1-16, doi:10.1002/jgrd.50177, 2013.

Harig, C., and Simons, F. J.: Accelerated West Antarctic ice mass loss continues to outpace East Antarctic gains. Earth Planet. Sci. Let. 415, 134-141, doi:10.1016/j.epsl2015.01.029, 2015.

691 Hirasawa, N., Nakamura, H., annd Yamanouchi, T.: Abrupt changes in meteorological
692 conditions observed at an inland Antarctic station in association with wintertime blocking.
693 Geophys. Res. Let., 27(13), 1911-1914, 2000.

694 Hirasawa, N., Nakamura, H., Motoyama, H., Hayashi, M., and Yamanouchi, T.: The role of
695 synoptic-scale features and advection in a prolonged warming and generation of different
696 forms of precipitation at dome Fuji station, Antarctica, following a prominent blocking event,
697 J. Geophys. Res., 118, 6916-6928, doi:10.1002/jgrd.50532, 2013.

698 Jouzel, J., Vimeux, F., Caillon, N., Delaygue, G., Hoffmann, G., Masson-Delmotte, V., and
699 Parrenin, F.: Magnitude of isotope/temperature scaling for interpretation of central Antarctic
700 ice cores, J. Geophysic. Res., 108 (D12), 4361, doi:10.1029/2002JD002677, 2003.

701 Jouzel, J., in: Heinrich Holland and Karl Turekian (Ed.) Treatise on Geochemistry (Second
702 Edition) 5.8, Elsevier, 213-256, 2014.

703 Karoly, D. J.: Southern Hemisphere circulation features associated with El Nino-Southern
704 Oscillation events, J. Clim., 2, 1239-1251, 1989.

705 King, J. and Turner, J.: Antarctic Meteorology and Climatology. Cambridge Atmospheric and
706 Space Sciences Series, Cambridge University Press, Cambridge, 409pp, 1997.

707 Lenaerts, J. T. M., van Meijgaard, E., Van den Broeke, M.R., Ligtenberg, S. R. M., Horwarth,
708 M., and Isaksson, E.: Recent snowfall anomalies in Dronning Maud Land, East Antarctica, in
709 a historical and future climate perspective. Geophys. Res. Let., 40, 2684-2688,
710 doi:10.1002/grl.50559, 2013.

711 Lorius, C., Merlivat, L., Jouzel, J., and Pourchet, M.: A 30,000 years isotope climatic record
712 from Antarctic ice, Nature, 280, (5724), 644-647, 1979.

713 Marshall, G. J.: Trends in the Southern Annular Mode from observations and reanalyses, J.
714 Clim., 16**,** 4134-4143, 2003.

715 Marshall, G. J., : Half-century seasonal relationship between the Southern Annular Mode and
716 Antarctic temperatures, Int. J. Climatol., 27, 373-383, 2007.

717 Massom, R., Pook, M. J., Comiso, J. C., Adams, N., Turner, J., Lachlan-Cope, T., and Gibson,
718 T.: Precipitation over the interior East Antarctic ice sheet related to midlatitude blocking-high
719 activity. J. Climate, 17, 1914-1928, 2004.

Monaghan, A. J., Bromwich, D. H., Powers, J. G., Manning, K. W.: The Climate of McMurdo, Antarctica, Region as Represented by One Year of Forecasts from the Antarctic Mesoscale Prediction System, J. Climate, 18, 1174-1189, 2005.

Monaghan, A. J., Bromwich, D. H., Fogt, R. L., Wang, S., Mayewski, P. A.,Dixon, D. A., Ekaykin, A., Frezzotti, M., Goodwin, I., Isaksson, E., Kaspari, S. D., Morgan, V. I., Oeter, H., Van Ommen, T. D., Van der Veen, C. J., and Wen, J.: Insignificant change in Antarctic snowfall since the International Geophysical Year. Science, 313, 827-831, doi: 10.1126/science.1128243, 2006.

Nicolas, J. P. and Bromwich, D. H.: Climate of West Antarctica and Influence of Marine Air Intrusions. *J. Climate*, 24, 49-67. doi:10.1175/2010JCLI3522.1, 2011.

Nigro, M. A., Cassano, J. J., and Seefeldt, M. W.: A weather pattern-based approach to evaluate the Antarctic Mesoscale Prediction System (AMPS) forecasts: Comparison to automatic weather station observations. Wea. Forecasting, 26, 184–198, doi:10.1175/2010WAF2222444.1, 2011.

Nigro, M. A., Cassano, J. J., and Knuth, S. L.: Evaluation of Antarctic Mesoscale Prediction System (AMPS) cyclone forecasts using infrared satellite imagery. Antarctic Science, 24, 183-192, doi:10.1017/S0954102011000745, 2012.

Noone, D., and Simmonds, I.: Implications for the interpretation of ice-core isotope data from analysis of modelled Antarctic precipitation. Ann. Glaciol., 27, 398-402, 1998.

Noone, D., and Simmonds, I.:Associations between $\delta^{18}O$ Of water and climate parameters in a simulation of atmospheric circulation for 1979-95. J. Clim., 15, 3150-3169, 2002.

Noone, D., Turner, J., and Mulvaney, R.: Atmospheric signals and characteristics of accumulation in Dronning Maud Land, Antarctica. J. Geophysic. Res., 104 (D16), 19,191-19,211, 1999.

Nygard, T., Valkonen, T., and Vihma, T.: Antarctic Low-Tropopause Humidity Inversions: 10-yr Climatology, J. Climate, 26, 5205-5219, doi: 10.1175/JCLI-D-12-00446.1, 2013.

Powers, J. G., Monaghan, A. J, Cayette, A. M., Bromwich, D. H., Kuo, Y., and Manning, K. W.: Real-time mesoscale modeling over Antarctica. The Antarctic Mesoscale Prediction System. Bull. Am. Meteorol. Soc., 84, 1522-1545, 2003.

749 Powers, J. G.: Numerical prediction of an Antarctic severe wind event with the Weather
750 Research and Forecasting (WRF) Model. Mon. Wea. Rev., 135, 3134-3157, 2007.

751 Powers, J. G., Manning, K. W., Bromwich, D. H., Cassano, J. J., and Cayette, A. M.: A decade
752 of Antarctic science support through AMPS. Bull. Amer. Meteor. Soc., 93, 1699-1712, 2012.

753 Raphael, M. N.: A zonal wave 3 index for the Southern Hemisphere, Geophys. Res. Let.,
754 31(23), doi:10.1029/2004GL020365, 2004.

755 Reijmer C. H, Van den Broeke, M. R., and Scheele, M. P.: Air parcel trajectories and snowfall
756 related to five deep drilling locations in Antarctica based on the ERA-15 dataset, J. Climate,
757 15:1957–1968, 2002.

758 Reijmer, C. H. and van den Broeke, M. R.: Temporal and spatial variability of the surface
759 mass balance in Dronning Maud Land, Antarctica. J. Glaciol., 49(167), 512-520, 2003.

760 Ritter, F., Steen-Larsen, H. C., Kipfstuhl, J., Orsi, A., Behrens, M., and Masson-Delmotte, V.:
761 First continuous measurements of water vapor isotopes on the Antarctic Plateau, Geophys.
762 Res. Abstr., 16, EGU2014-9721, 2014.

763 Scarchilli, C., Frezzotti, M., and Ruti, P. M.: Snow precipitation at four ice core sites in East
764 Antarctica - provenance, seasonality and blocking factors. Clim. Dyn., 37, 2107-2125,
765 doi:10.1007/s00382-010-0946-4, 2010.

766 Schlosser, E.: Effects of seasonal variability of accumulation on yearly mean $\delta^{18}O$ values in
767 Antarctic snow, *J. Glaciol.* , 45 (151), 463-468, 1999.

768 Schlosser, E., Duda, M. G., Powers, J. G, Manning, K. W.: The precipitation regime of
769 Dronning Maud Land, Antarctica, derived from AMPS (Antarctic Mesoscale Prediction
770 System) Archive Data. J. Geophys. Res., 113. D24108, doi: 10.1029/2008JD009968, 2008.

771 Schlosser, E., K. W. Manning, K. W., Powers, J. G., Duda, M. G., Birnbaum, G., and Fujita,
772 K.: Characteristics of high-precipitation events in Dronning Maud Land, Antarctica. J.
773 Geophys. Res., 115, D14107, doi:10.1029/2009JD013410, 2010.

774 Schlosser, E., Powers, J. G., Duda, M. G., Manning, K. W., Reijmer, C.H., Van den Broeke,
775 M.: An extreme precipitation event in Dronning Maud Land, Antarctica - a case study using
776 AMPS (Antarctic Mesoscale Prediction System) archive data. Polar Research,
777 doi:10.1111/j.1751-8369.2010.00164.x, 2010.

778 Schlosser, E., Manning, K. W., Powers, J. G., Gillmeier, S., and Duda, M. G., An extreme
779 precipitation/warming event in Antarctica – a study with Polar WRF, in preparation, 2016.

780 Sodemann, H, and A Stohl. 2009. Asymmetries in the moisture origin of Antarctic
781 precipitation. Geophys.Res. Letters 36: L22803. doi:10.1029/2009GL040242.
782
783 Sodemann, H., Masson-Delmotte, V., Schwierz, C., Vinther, B. M. and Wernli, H.,: Inter-
784 annual variability of Greenland winter precipitation sources. Part II: Effects of North Atlantic
785 Oscillation variability on stable isotopes in precipitation, J. Geophys. Res., 113, D12111,
786 doi:10.1029/2007JD009416, 2008.

787 Schwerdtfeger, W.: Weather and Climate of the Antarctic. Elsevier Science Publishers,
788 Amsterdam-London-New York-Tokyo. 262pp, 1984.

789 Seefeldt, M. W., and Cassano, J. J.: An analysis of low-level jets in the greater Ross Ice Shelf
790 region based on numerical simulations. *Mon. Wea. Rev.*, **136**, 4188-4205. doi:
791 10.1175/2007JAMC1442.1, 2008.

792 Seefeldt, M. W., and Cassano, J. J.: A description of the Ross Ice Shelf air stream (RAS)
793 through the use of self-organizing maps (SOMs). *J. Geophys. Res.*, **117**, D09112.
794 doi:10.1029/2011JD016857, 2012.

795 Simmonds, I., Keay, K., and Lim, E.: Synoptic activity in the seas around Antarctica. Mon.
796 Wea. Rev., 131, 272-288, 2002.

797 Sinclair, M. R.: Record-high temperatures in the Antarctic – A synoptic case study, Mon. Wea.
798 Rev., 109, 2234- 2242, 1981.

799 Skamarock, W. C., Klemp, J. B., Dudhia, J., Gill, D. O., Barker, D. M., Duda, M. G., Huang,
800 X., Wang, W, and Powers, J. G.: A description of the Advanced Research WRF Version 3,
801 NCAR/TN 475+STR, 125 pp., Nat. Cent. for Atmos. Res., Boulder, Co, 2008.

802 Stenni, B., Masson-Delmotte, V., Johnsen, S., Jouzel, J., Longinelli, A., Monnin, E.,
803 Roethlisberger, R., and Selmo, E.: An Oceanic Cold Reversal During the Last Deglaciation,
804 Science, 293, 2074-2077, 2001.

805 Stenni, B., Masson-Delmotte, V., Selmo, E., Oerter, H., Meyer, H., Roethlisberger, R., Jouzel,
806 J., Cattani, O., Falourd, S., Fischer, H., Hoffmann, G., Iacumin, P., Johnsen, S. F., Minster, B.,

807 and Udisti, R.: The deuterium excess records of EPICA Dome C and Dronning Maud Land
808 ice cores (East Antarctica), Quat. Scie. Rev., 29, 146-159, 2010.

809 Stenni, B., Bonazza, M., Cagnati, A. Cattani, F., Dreossi, G., Frezzotti, M., Frosini,D.,
810 Grigioni, P., Karlicek, D., Masson-Delmotte, V., Scarchilli, C., Risi, C., Schlosser, E., Udisti,
811 R., and Valt, M.: Three year monitoring of stable isotopes of precipitation at Dome Concordia,
812 Antarctica. To be submitted to GRL, asap, 2015

813 Steen-Larsen, H. C. , S. J. Johnson, S. J., Masson-Delmotte, V., Stenni, B., Risi, C.,
814 Sodemann, H., Balslev-Clausen, D., Blunier, T., Dahl-Jensen, D., Ellehøy, M. D., Falourd, S.,
815 Grindsted, A., Gkinis, V., Jouzel, J., Popp, T., Sheldon, S., Simonsen, S. B., Sjolte, J.,
816 Steffensen, J. P., Sperlich, P., Sveinbjörnsdottir, A. E., Vinther, B. M., White, J. W. C.:
817 Continuous monitoring of summer surface water vapor isotopic composition above the
818 Greenland Ice Sheet, Atmos. Chem. Phys., 13, 4815-4828, 2013.

819 Stoelinga, M. T.: A users guide to RIP Version 4.5: A program for visualizing mesoscale
820 model output. NCAR online document. University of Washington.
821 http://www2.mmm.ucar.edu/wrf/users/docs/ripug.htm., 2009.

822 Suzuki, K., Yamanouchi, T., and Motoyama, H.: Moisture transport to Syowa and Dome Fuji
823 stations in Antarctica, J. Geophys. Res., 113, D24 114, doi:10.1029/2008JD009794, 2008.

824 Thompson, D. W. J., and J. M. Wallace: Annular modes in the extratropical circulation. Part I:
825 Month-to-month variability, J. Climate, 13, 1000-1016.

826 Trenberth, K. E., and Mo, K. C.: Blocking in the Southern Hemisphere, Mon. Weather Rev.,
827 133, 38-53, 1985.

828 Van Loon, H.: The half-yearly oscillation in middle and high southern latitudes and the
829 coreless winter. J. Atmos. Sci., 24, 472-486, 1967.

830 Van Loon, H., and Jenne, R. L., The zonal harmonic standing waves in the Southern
831 Hemisphere, J. Geophys. Res., 77, 992-1003, 1972.

832 Winkelmann, R., Levermann, A., Martin, M. A., and Frieler, K.: Increased future ice
833 discharge from Antarctica owing to higher snowfall. Nature, 492, 239-242, 2012.

834

835

Figure Captions

Fig. 1

Map of Antarctica indicating Dome C and other important deep-drilling sites in Antarctica

Fig. 2

AMPS domains used for model output analysis in this study

Fig. 3

a) Mean monthly temperatures for 2009 and 2010 at Dome C AWS

b) Daily precipitation and daily mean temperature at Dome C for 2009 and 2010

Fig. 4

Monthly precipitation at Dome C a) 2009 and b) 2010, distinguishing three different types of precipitation: diamond dust, hoar frost, and snowfall

Relative frequency of diamond dust, hoar frost, and snowfall for c) 2009 and d) 2010

The types were determined from photos of the crystals on the platforms by the Avalanche Research Institute, Arabba, Italy.

Fig. 5

a) 500hPa geopotential height from AMPS archive data (Domain 1) 13.9.2009 00Z

(The axis of the upper-level ridge mentioned in the text is marked by a bold black line.)

b) 24h-precipitation from AMPS 13.9. 2009 00GMT to 24 GMT

c) 5-day back-trajectories for parcels arriving at Dome C at 0000UTC 12.9.2009. Trajectories for three arrival levels are shown: 1. 600hPa, 2. 500hPa, 3. 300hPa

Fig. 6

Example for synoptic situation, during which precipitation is observed at Dome C, but not forecast by WRF in AMPS.

a) 500 hPa geopotential height, Domain 2.

b) 24h-precipitation total (mm) from AMPS

Fig. 7

Mean July- 500hPa geopotential height based on AMPS archive model output for 2009 and 2010.

Fig. 8

Mean monthly SAM index for 2009 and 2010 (after Marshall, 2003).

Fig. 9

a) Monthly mean Zonal Wave Number 3 (ZW3) index for 2009-2010

b) July 2009 500hPa geopotential height anomaly: Mean July 2009 height minus long-term zonal mean height

c) July 2010 500hPa geopotential height anomaly: Mean July 2009 height minus long-term zonal mean height

Fig. 10

Daily mean air temperatures at Dome C 2009 and 2010 from AWS and stable isotopes ($\delta^{18}O$ and deuterium excess) of corresponding precipitation samples

Fig. 1

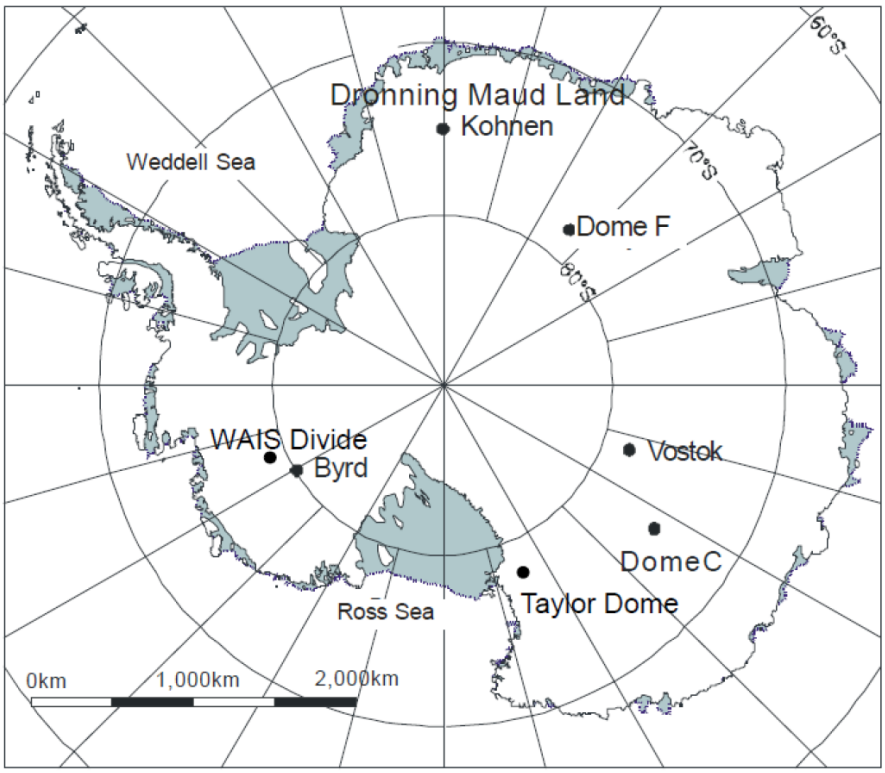
Dronning Maud Land
Kohnen
Weddell Sea
Dome F
60°S
70°S
80°S
WAIS Divide
Byrd
Vostok
DomeC
Taylor Dome
Ross Sea
0km
1,000km
2,000km

Fig. 2

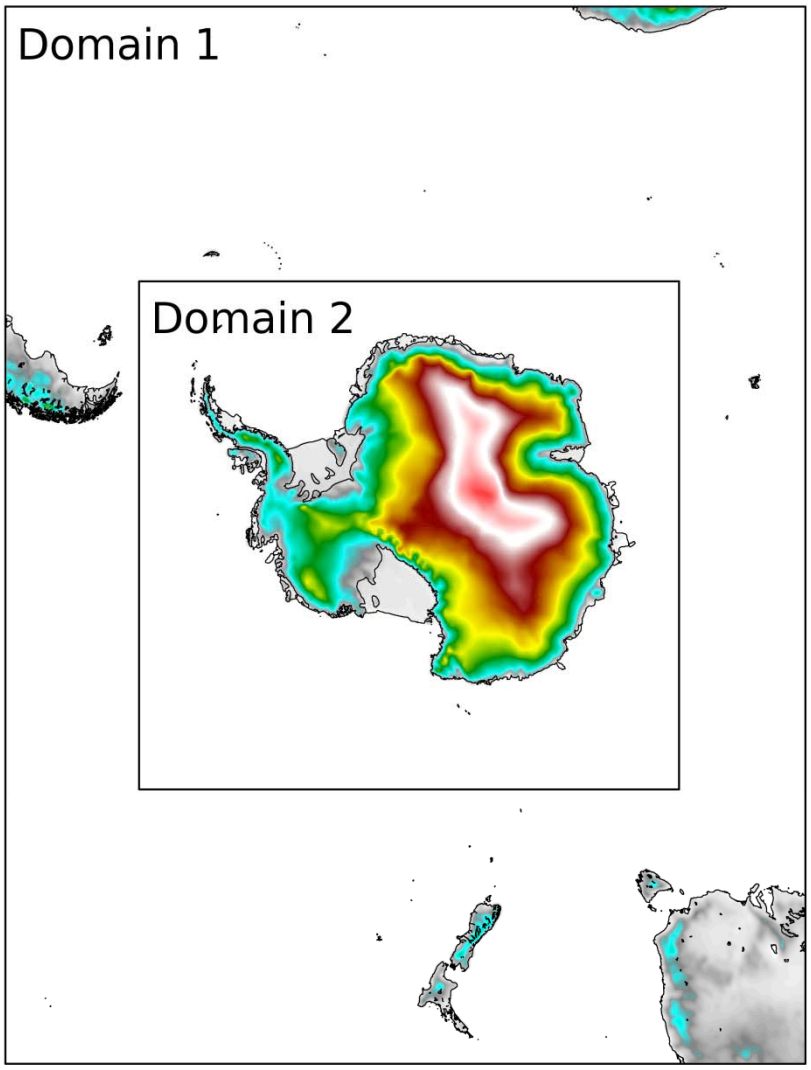

Fig. 3

a)

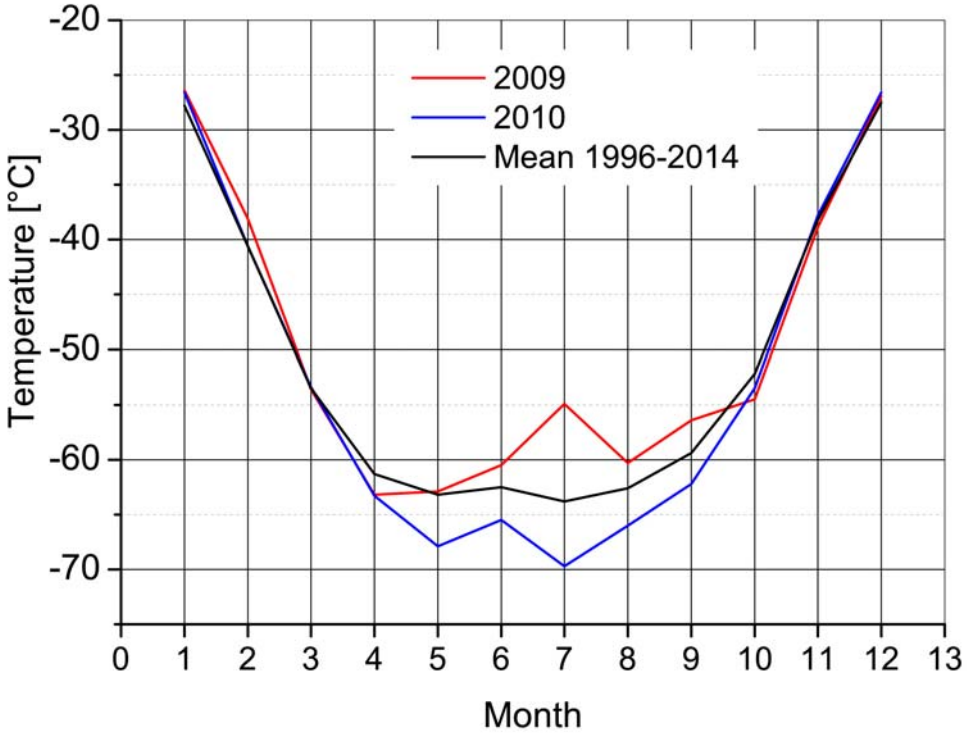
-20
-30
-40
-50
-60
-70
Temperature [°C]
0
1
2
3
4
5
6
7
8
9
10
11
12
13
Month
2009
2010
Mean 1996-2014

b)

2009

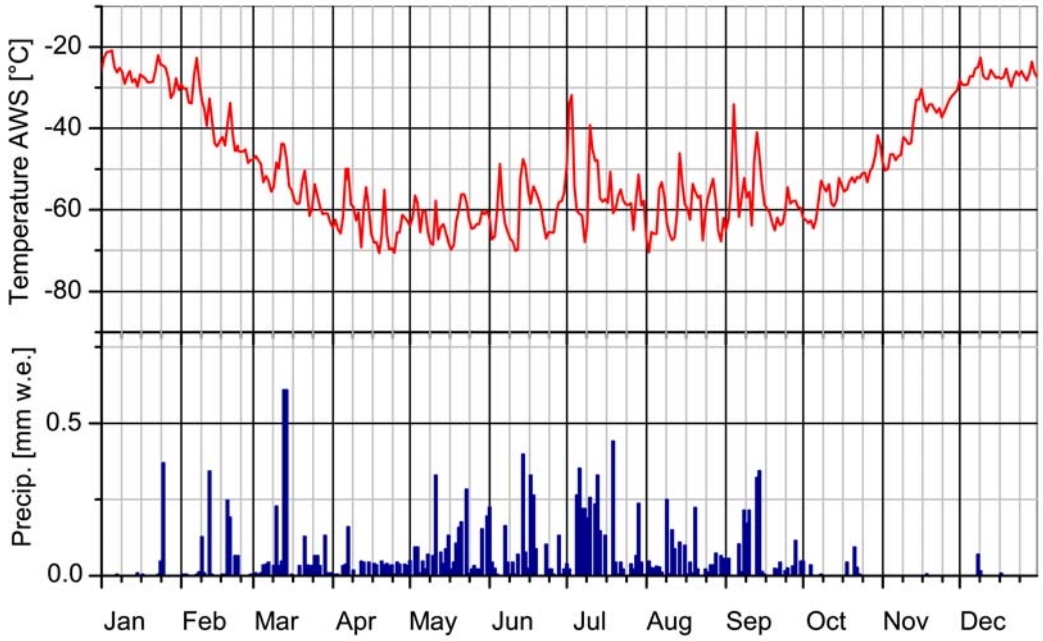
Temperature AWS [°C]
-20
-40
-60
-80
Precip. [mm w.e.]
0.5
0.0
Jan
Feb
Mar
Apr
May
Jun
Jul
Aug
Sep
Oct
Nov
Dec

2010

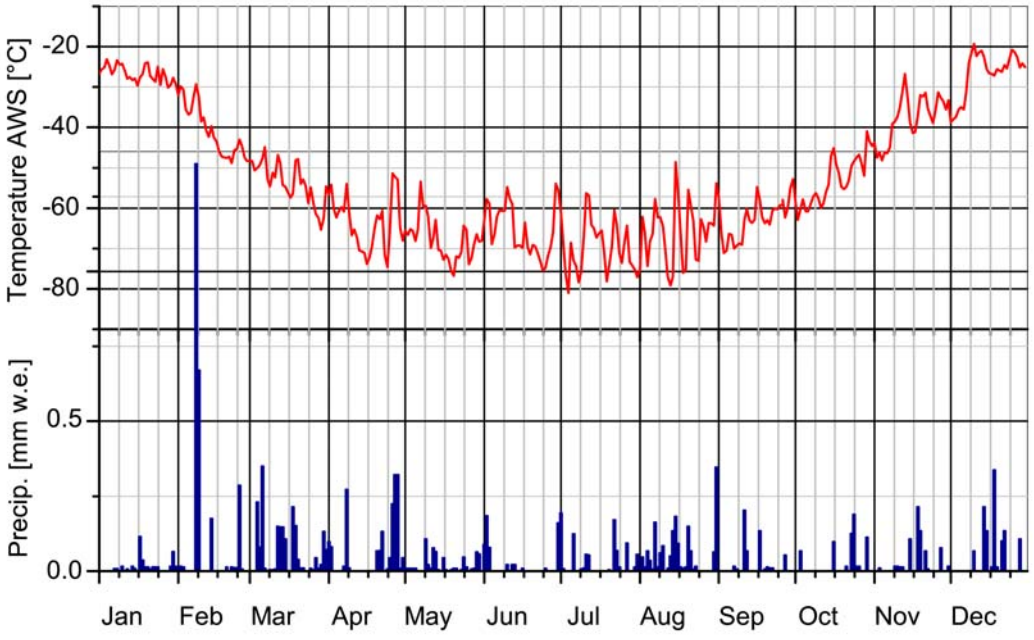
Temperature AWS [°C]
-20
-40
-60
-80
Precip. [mm w.e.]
0.5
0.0
Jan
Feb
Mar
Apr
May
Jun
Jul
Aug
Sep
Oct
Nov
Dec

Fig. 4

a)

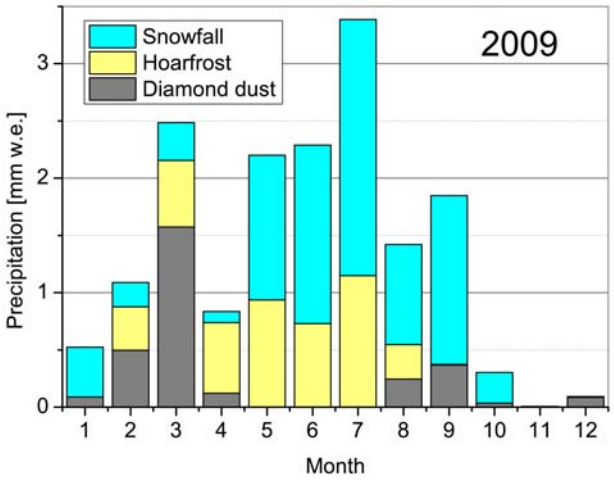
Snowfall
Hoarfrost
Diamond dust
2009
Precipitation [mm w.e.]
Month
0
1
2
3
1
2
3
4
5
6
7
8
9
10
11
12

b)

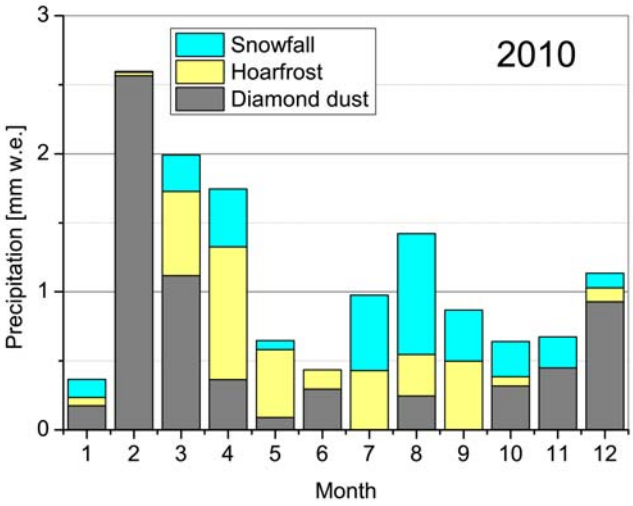
Snowfall
Hoarfrost
Diamond dust
2010
Precipitation [mm w.e.]
Month
0
1
2
3
1
2
3
4
5
6
7
8
9
10
11
12

c)

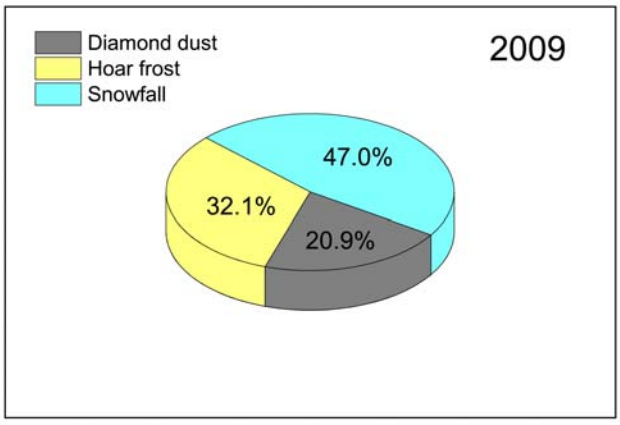
Diamond dust
Hoar frost
Snowfall
2009
47.0%
32.1%
20.9%

d)

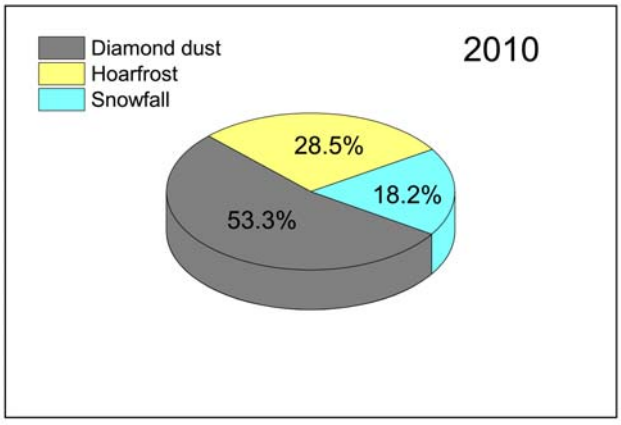
Diamond dust
Hoarfrost
Snowfall
2010
28.5%
18.2%
53.3%

961 **Fig. 5**

962 **a)**

963

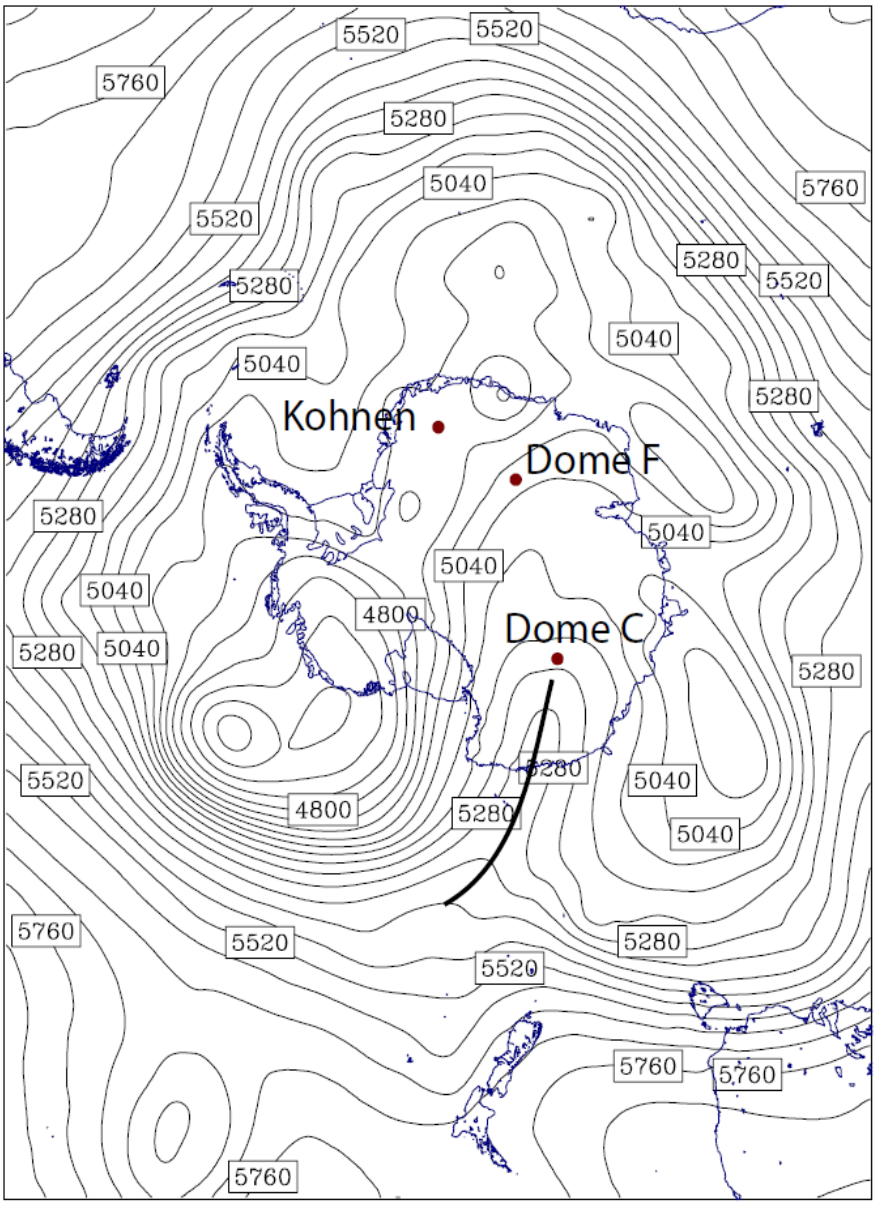

979

980

981

982

983

b)

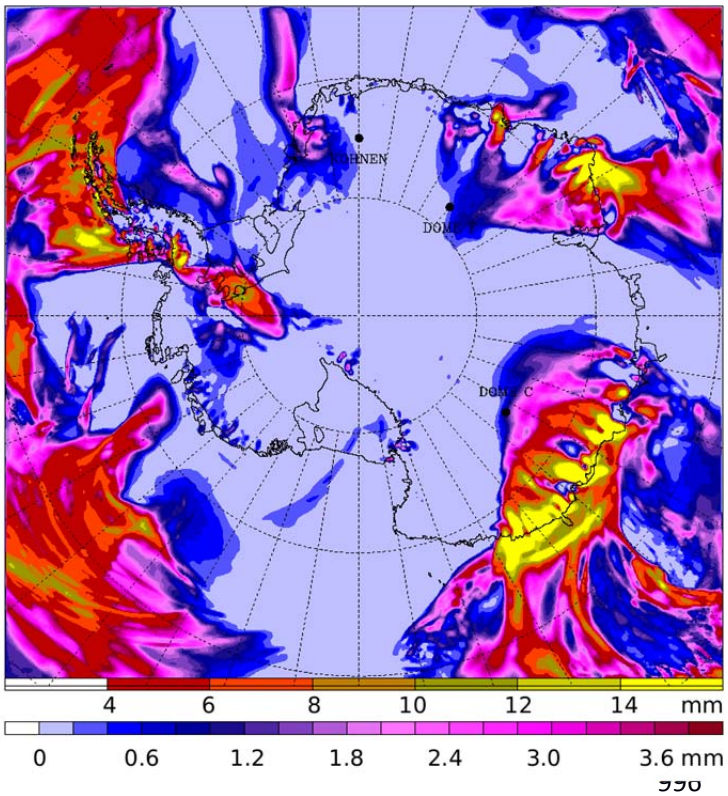
4
6
8
10
12
14
mm
0
0.6
1.2
1.8
2.4
3.0
3.6 mm

c)

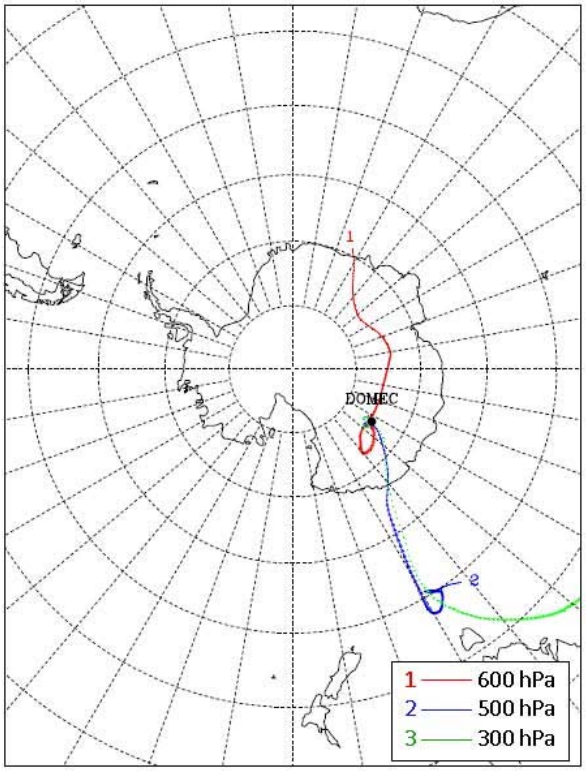
DOMEC
1
2
1 600 hPa
2 500 hPa
3 300 hPa

Fig. 6

a)

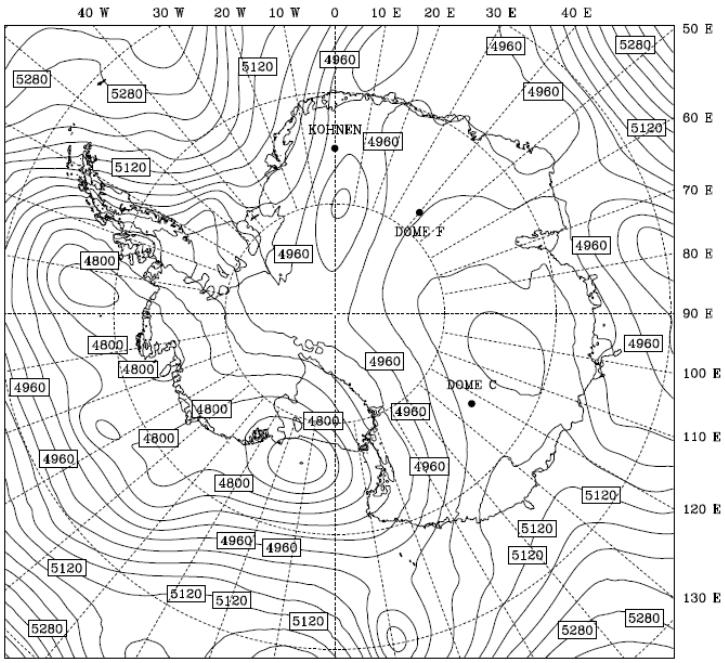
40 W
30 W
20 W
10 W
0
10 E
20 E
30 E
40 E
50 E
60 E
70 E
80 E
90 E
100 E
110 E
120 E
130 E
KOHNEN
DOME F
DOME C
4800
4960
5120
5280

b)

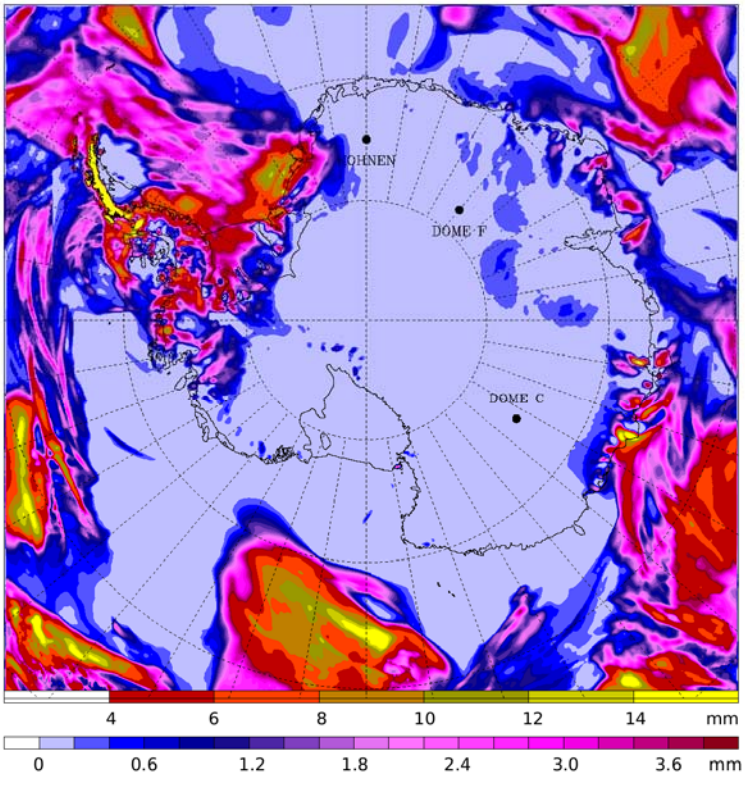
KOHNEN
DOME F
DOME C
4
6
8
10
12
14
mm
0
0.6
1.2
1.8
2.4
3.0
3.6
mm

Fig. 7

a) July 2009

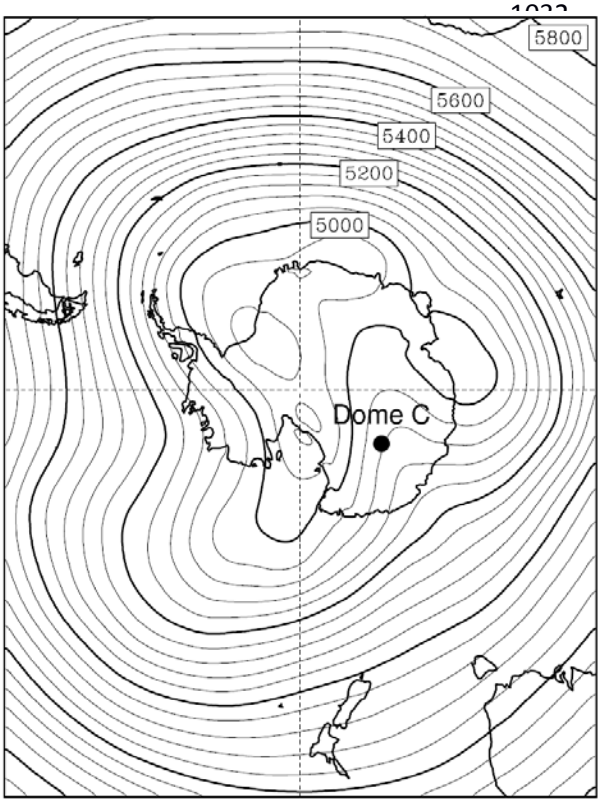

b) July 2010

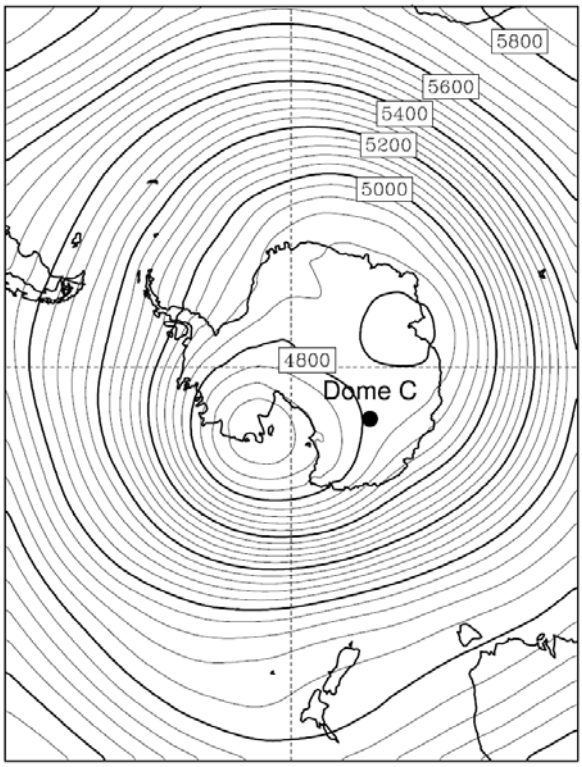

Fig. 8

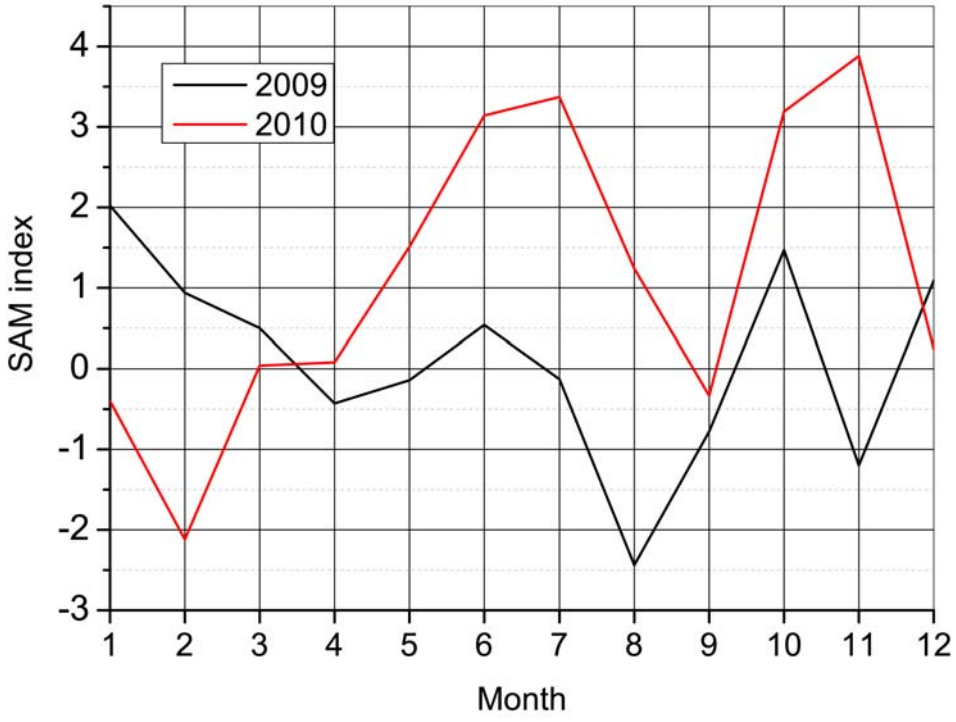

Fig. 9

a)

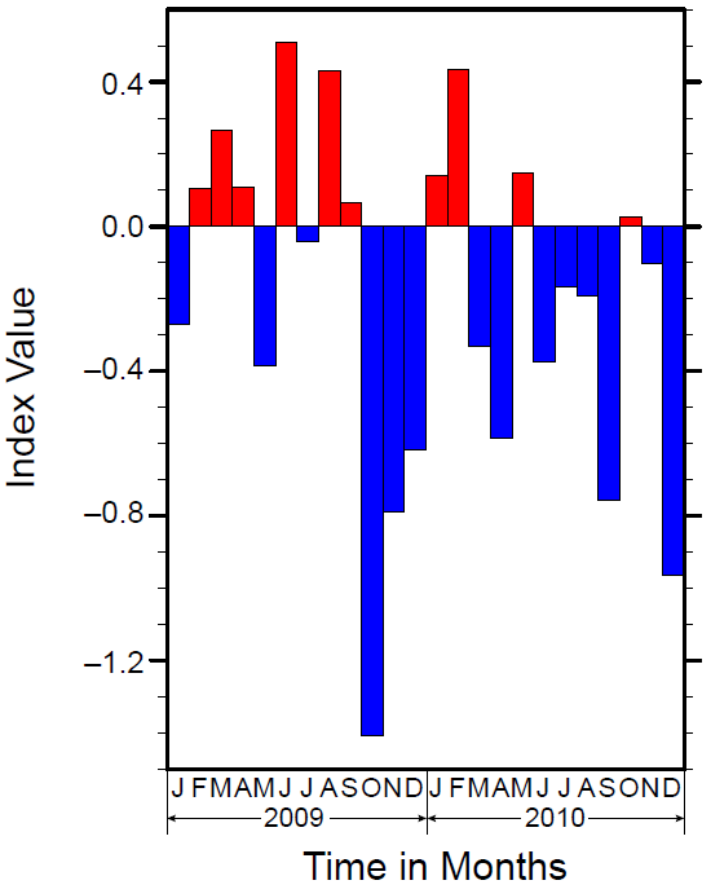
0.4
0.0
−0.4
−0.8
−1.2
Index Value
J FMAMJ J ASOND J FMAMJ J ASOND
2009
2010
Time in Months

b) 500hPa geopotential height: mean July 2009 minus long-term zonal mean

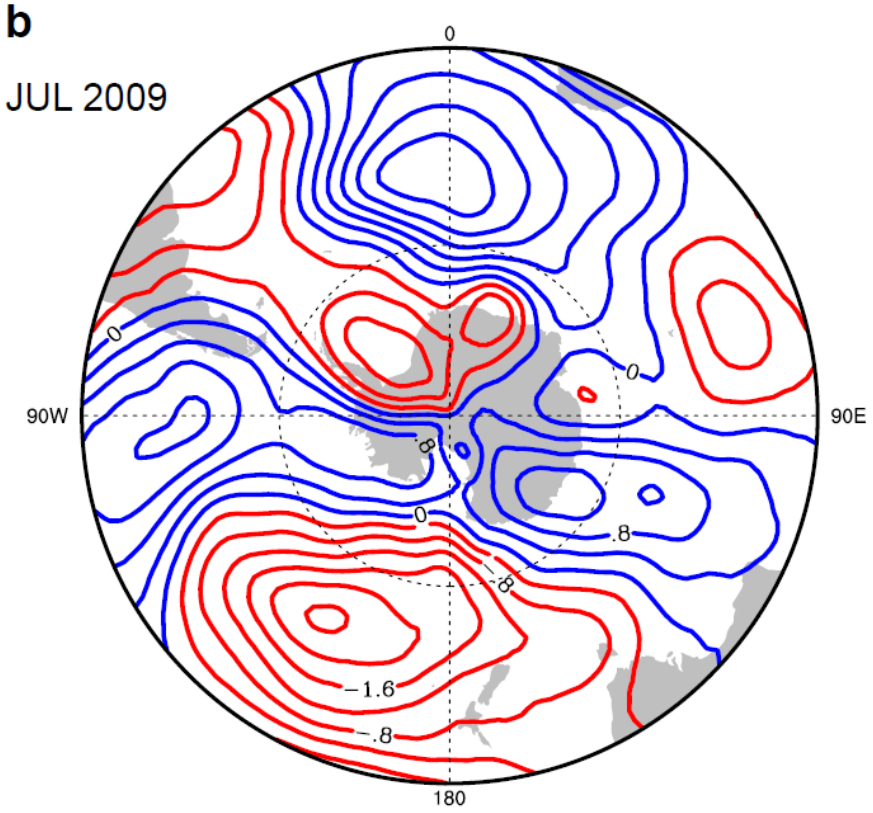

c) 500hPa geopotential height: mean July 2010 minus long-term zonal mean

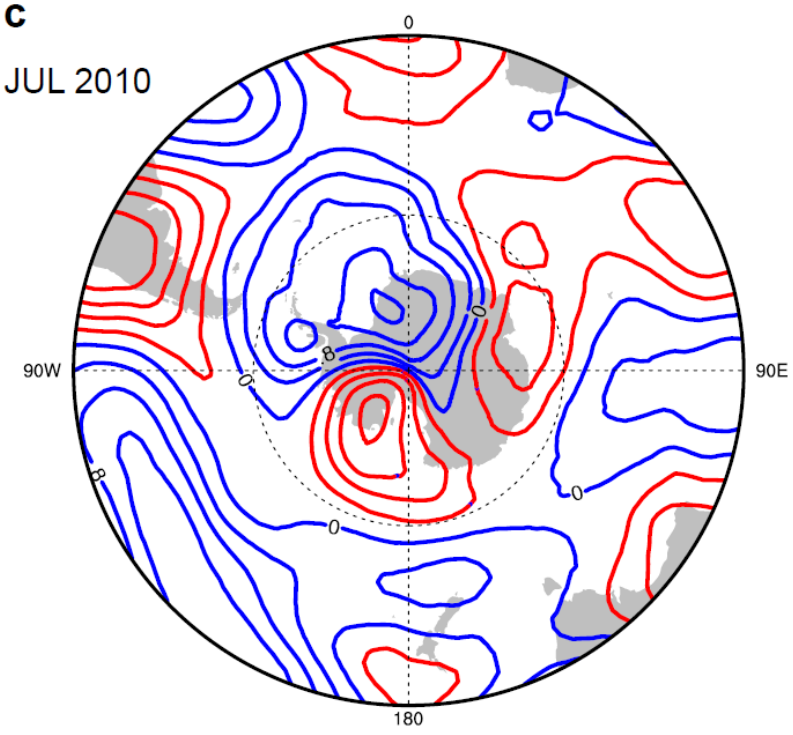

Fig. 10

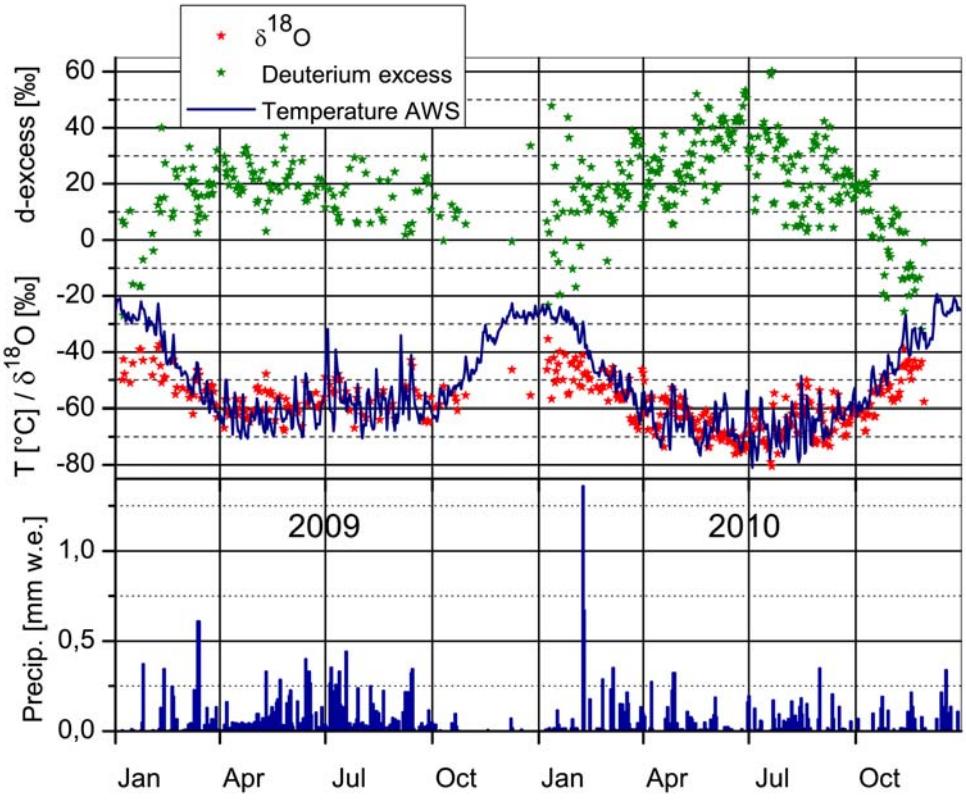

Remark: for d-excess we prefer not to use a capital letter in the axis title because commonly "d" is defined as deuterium excess whereas "D" means deuterium.